4.1. INTRODUCTION

Recently, BMNPs have received considerable attention because of their importance for magnetic, optical, and catalytic applications in a variety of fields [Pei *et al*., (2015); Wang *et al*., (2015); Lozano *et al*., (2013); Mishra *et al*., (2015); Xiang *et al*., (2015); Zhang *et al*., (2013)]. Their value arises from their distinctive properties, which are clearly different from those of monometallic nanoparticles [Tao *et al*, (2008); Ferrando *et al*, (2008); Burda *et al*, (2005)]. The BMNPs are also an attractive target of catalytic research because their potential properties, such as selectivity of catalytic reactions, chemical and physical stability are distinct from those of the component monometallic nanoparticles. A variety of method has been reported for the synthesis of BMNPs [Scott *et al*, (2004); Park *et al*, (2008); Tokonami *et al*., (2010); Zhang *et al*., (2013); Lazarus *et al*., (2012); Li *et al*., (2014); Hutchings and Kiely., (2013); Sankar*et al*., (2012)]. The common method of the synthesis of BMNPs are chemical reduction, [Scott., (2015);], photolytic reduction [Gonzalez *et al*., (2014)], radiolytic reduction [Mallik *et al*., (2001); Esfahani *et al*., (2010); Hai *et al*., (2014);], metal evaporation [Villa *et al*., (2015)] and sonochemical synthesis [Mizukoshi *et al*., (1997); Kan *et al*., (2003); Anandan *et al*., (2008)]. Apart from these, there is a need of synthesis of stabilized functional BMNPs under ambient conditions remains a challenge from following aspects: (1) stability and processability for nanocomposite formation; (2) functional ability and biocompatibility for specific applications. The synthesis of BMNPs by chemical reduction methods is therefore often performed in the presence of various functionalized stabilizers in order to prevent unwanted agglomeration of the colloidal BMNPs. Accordingly there is a requirement of suitable reagents that not only acts as reducing agent but also efficiently stabilized the BMNPs.

The findings reported in Chapter three and four described the synthesis of monometallic nanoparticles (AgNPs and PdNPs) involving the active role of GPTMS, Cyclohexanone, Formaldehyde and THF-HPO from 3-APTMS capped noble metal ions. The role of these organic reagents during the formation of BMNPs (Pd-Au/Au-

Pd and Ag-Au/Au-Ag) has been studied herein. We report the process for the synthesis of Au-Pd/Pd-Au and Ag-Au/Au-Ag BMNPs through organic mediated reduction of 3-APTMS capped metal ions present in desired ratio. The Pd-Au/Au-Pd has been made following two different reaction protocol namely: Simultaneous and Sequential. In Simultaneous method, co-complexation of both precursor metal ions followed by simultaneous reduction is made. In Sequential method monometallic nanoparticles is made first followed by allowing the reduction of second metal from similar reducing agent however, Ag-Au/Au-Ag are made following simultaneous protocol. In both cases the metal ions are initially treated with 3-APTMS followed by reduction through organic reducing agents. Two different reducing agents namely: THF-HPO and Cyclohexanone are used for the synthesis of Pd-Au/Au-Pd and Ag-Au/Au-Ag respectively. These BMNPs have been used for making nanocomposites of PBNPs.

Nanocomposites are a rapidly growing area of research in advanced functional materials science. The properties of nanocomposite materials depend not only on the properties of their individual constituents, but also on their morphology and interfacial characteristics. The surface modification, functionalization of nanoparticles, covalent attachment, self-assembly, and ease of organization on the surfaces provide a means to generate nanocomposite materials with tunable surface properties. As an example, a nanocomposite with Prussian blue is made and found to exhibit unusual property combinations and unique design possibilities. Accordingly, tuning ability of the AgNPs and Au-AgNPs with PBNPs leading to the formation of nanocomposites has been investigated. Similar reducing agents are used for the synthesis of both AgNPs, Au-AgNP and PBNPs. The choice of appropriate composition yielded the tuning into the nanocomposite formation having wider applications in both homogeneous and heterogeneous catalysis.

4.2. EXPERIMENTAL

4.2.1. Materials

3-aminopropyltrimethoxysilane (3-APTMS), 3-glycidoxypropyltrimethoxysilane (GPTMS), silver nitrate ($AgNO_3$), potassium tetrachloropalladate (II) [K_2PdCl_4] and tetrachloroauric acid ($HAuCl_4$) were obtained from Aldrich Chemical Co., India. Potassium ferricyanide and cyclohexanone were obtained from Merck, India. Tetrahydrofuran hydroperoxide (THF-HPO) was synthesized by autoxidation of THF. All other chemical employed were of analytical grade.

4.2.2. Preparation of Bimetallic Nanoparticles (BMNPs)

4.2.2.1. Synthesis of bimetallic Pd-Au/Au-Pd made through THF-HPO and 3-APTMS

The preparation of bimetallic nanoparticles involves both simultaneous and sequential reduction of known ratio of metal salts. Pd-Au is made using K_2PdCl_4 and $HAuCl_4$ in 4:1 ratio whereas Au-Pd is made using 1:4 ratios of the same. In simultaneous process for Pd-Au synthesis involves the mixing of 80 μL aqueous solution of K_2PdCl_4 (0.003 M) and 20 μL aqueous solution of $HAuCl_4$ (0.01 M) under stirred condition followed by the addition of 10 μL of 3-APTMS (0.5 M) and 10 μL of THF-HPO. The reaction mixture was turned into blackish-red within 2 h. Whereas the Au-Pd under simultaneous process was made as follows: 80 μL aqueous solution of $HAuCl_4$ (0.01 M) was mixed with 20 μL aqueous solution of K_2PdCl_4 (0.003 M) under stirring condition, followed by the addition of 10 μL of 3-APTMS (0.5 M) and 10 μL of THF-HPO. After this, the color of NPs turned to reddish-black, indicating the formation of Au-Pd. In sequential method the synthesis of Pd-Au involves the mixing of 80 μl aqueous solution of K_2PdCl_4 (0.003 M) and 10 μl of 3-APTMS (0.5 M) followed by addition of 10 μl of THF-HPO under stirred condition. The

reaction mixture was turned to black color after 1 h. To this 20 μl of 3-APTMS capped $HAuCl_4$ (0.01 M) was added that enabled the formation of blackish-red color of Pd-Au within 2 h. Similarly, the sequential formation of Au-Pd involves the mixing of 80 μl aqueous solution of $HAuCl_4$ (0.01 M) and 10 μl of 3-APTMS (0.5 M) under stirred condition followed by the addition of 10 μl of THF-HPO. The reaction mixture was turned to red color after 1 h which was followed by the addition of 20 μl of 3-APTMS capped K_2PdCl_4 resulting the formation of reddish-black color of Au-Pd within 2 h. All the synthesis was performed at room temperature.

4.2.2.2. Cyclohexanone and 3-APTMS mediated synthesis of Ag-Au/Au-Ag

The preparation of bimetallic nanoparticles involves a known ratio of metal salts in which Ag–Au is made using $AgNO_3$ and $HAuCl_4$ in 4/1 ratio. The Ag–Au synthesis involves the mixing of 12 μL methanolic solution of $AgNO_3$ (0.025 M) and 12 μL methanolic solution of $HAuCl_4$ (0.0025 M) under stirred condition followed by the addition of 06 μL of 3-APTMS (0.5 M) and 10 μL of cyclohexanone. The reaction mixture turned dark yellow within 2 h. Whereas Au–Ag is made using $HAuCl_4$ and $AgNO_3$ in 4/1 ratio and the synthesis involves the mixing of 12 μL methanolic solution of $HAuCl_4$ (0.025 M) and 12 μL of methanolic solution of $AgNO_3$ (0.0025 M) under stirred condition followed by the addition of 06 μL of 3-APTMS (0.5 M) and 10 μL of cyclohexanone. The reaction mixture turned purple within 1 h.

4.2.2.3.Synthesis of Nanocomposites of PBNP-AgNP/ PBNP-Au-Ag

PBNPs were synthesized as described earlier [Pandey and Pandey., (2013a)]. Nanoparticles decorated PBNP (PBNP–AgNPs and PBNP–Au–Ag) nanocomposites were prepared by careful mixing of as synthesized $AgNP_1$, $AgNP_4$, $AgNP_5$, Au–Ag and PBNPs. $AgNP_1$, $AgNP_4$ and $AgNP_5$ as discussed in Chapter 2 [sections 2.2.2.1 (Table 2.1) and 2.2.2.2.(2.2)]. AgNPs/Au–Ag (15μL) and PBNPs (5μL) under ambient conditions and left undisturbed for 5 minutes at room temperature (25^oC).

4.2.3. Measurements and Characterizations

The UV-Vis absorption spectra of samples were recorded in corresponding nanomaterials using a Hitachi U-2900 Spectrophotometer. Transmission electron microscopy (TEM) studies were performed using 200 kV and Philips CM 200 Supertwin TEM. Aqueous solutions were prepared by using doubly distilled-deionized water (Alga water purification system).

4.3. RESULTS

4.3.1. THF-HPO and 3-APTMS mediated synthesis of Pd-Au and Au-Pd

3-APTMS and THF-HPO enable the synthesis of PdNPs as discussed in Chapter 3. In addition to that the process also enables the synthesis of BMNPs of palladium and gold of variable ratio under two different conditions of reacting system: (a) simultaneous and (b) sequential. Figure 4.1 shows the visual photographs of Au-PdNPs and Pd-AuNPs made through 3-APTMS and THF-HPO mediated simultaneous conversion of respective noble metal salts. Subsequently a comparative study on the synthesis of bimetallic nanoparticles through simultaneous and sequential methods was made. The results of bimetallic nanoparticles as a function of time through simultaneously and sequentially using 80:20 ratio of K_2PdCl_4 and $HAuCl_4$ (Pd-Au) and 80:20 ratio of $HAuCl_4$ and K_2PdCl_4 (Au-Pd) as shown in Figure 4.2-5.

Figure 4.6 and 4.7 shows the SAED pattern of as synthesized Pd-Au and Au-Pd (simultaneous) and Figure 4.8 and 4.9 shows the SAED pattern of as synthesized Pd-Au and Au-Pd (sequential). Figure 4.10and 4.11 shows the TEM images of simultaneously synthesized Pd-Au and Au-Pd, while Figure 4.12 and 4.13 shows the sequentially synthesized Pd-Au and Au-Pd nanoparticles.

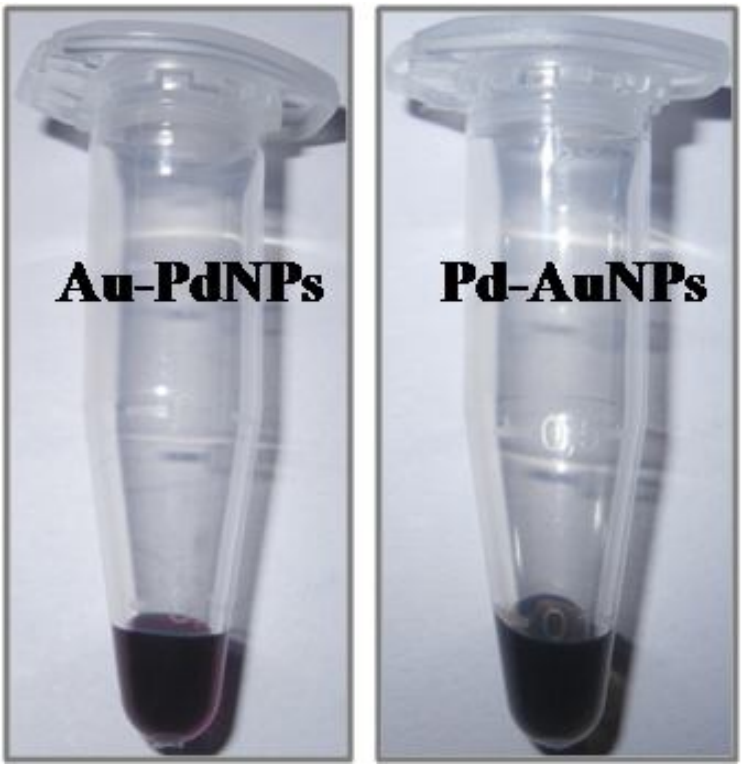

Figure. 4.1. The visual photographs of Au-PdNPs and Pd-AuNPs.

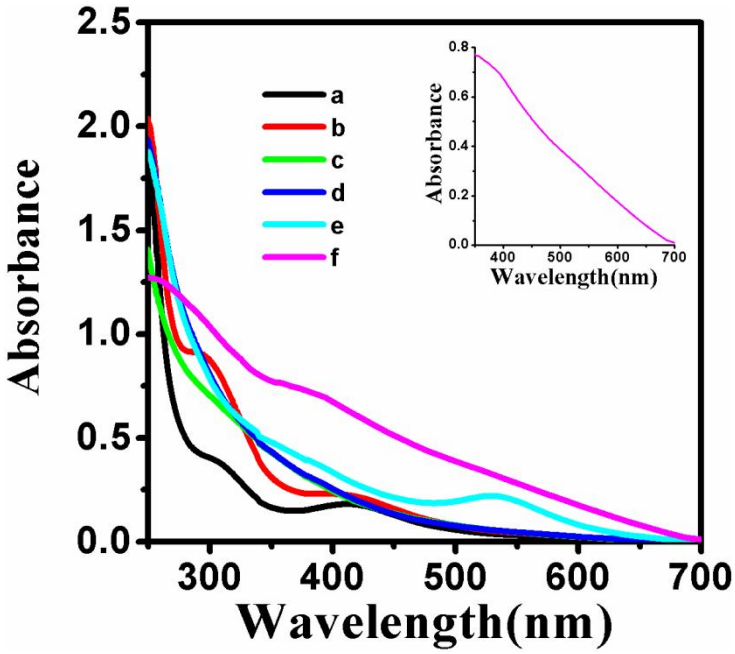

Figure. 4.2. UV-Vis spectra recorded on the simultaneous formation of Pd-Au from K_2PdCl_4 (80%) and $HAuCl_4$ (20%): the variation of absorbance as the function of wavelength on subsequent addition of K_2PdCl_4 (a), $HAuCl_4$ (b), 3-APTMS (c), THF-HPO (d), curve-e shows the absorbance recorded after 1 h from subsequent addition and curve-f shows the spectra recorded after simultaneous formation of Pd-Au.

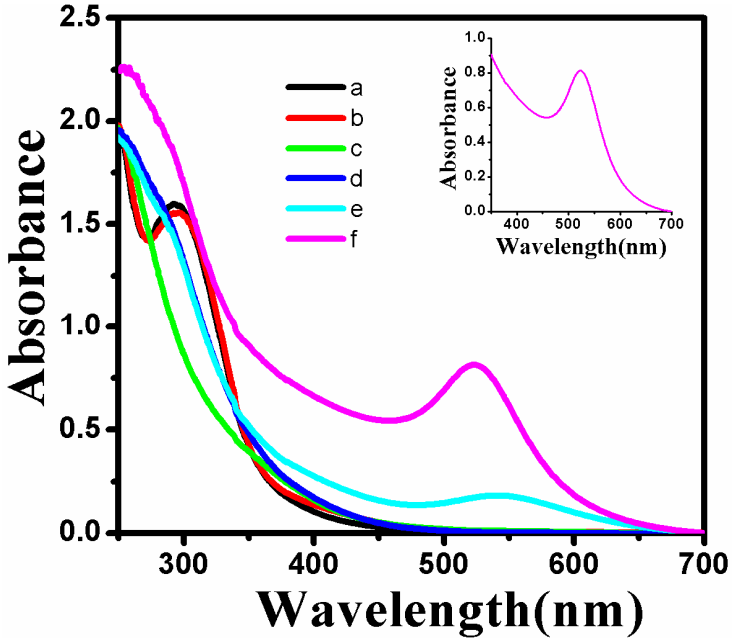

Figure. 4.3. UV-Vis spectra recorded on the simultaneous formation of Au-Pd from K_2PdCl_4 (20%) and $HAuCl_4$ (80%): the variation of absorbance as the function of wavelength on subsequent addition of K_2PdCl_4 (a), $HAuCl_4$ (b), 3-APTMS (c), THF-HPO (d), curve-e shows the absorbance recorded after 1 h from subsequent addition and curve-f shows the spectra recorded after simultaneous formation of Au-Pd.

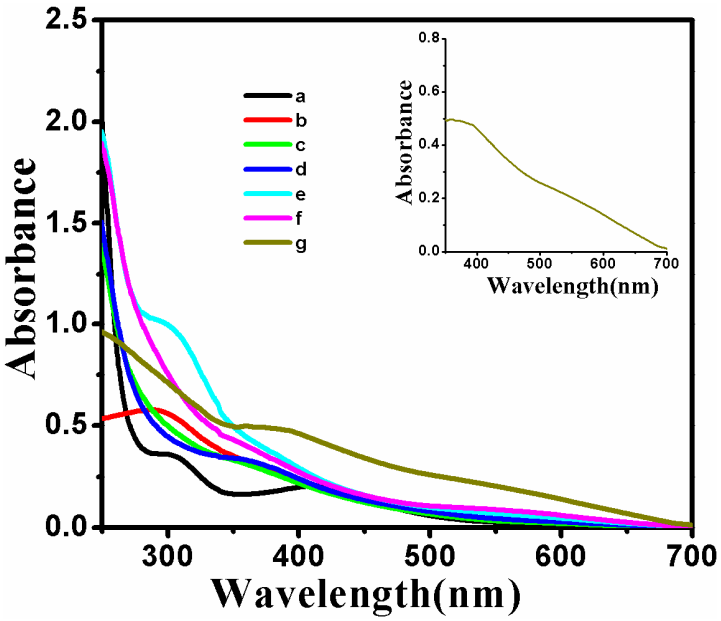

Figure. 4.4. UV-Vis spectra recorded on the sequential formation of Pd-Au from K_2PdCl_4 (80%) and $HAuCl_4$ (20%): the variation of absorbance of K_2PdCl_4 as a function of wavelength (a) followed by subsequent addition of 3-APTMS (b), THF-HPO (c), curve-d shows the spectra recorded after1 h, curve-e shows the absorption after subsequent addition of $HAuCl_4$ followed by addition of 3-APTMS (f), curve-g shows the spectra recorded after sequential formation of Pd-Au.

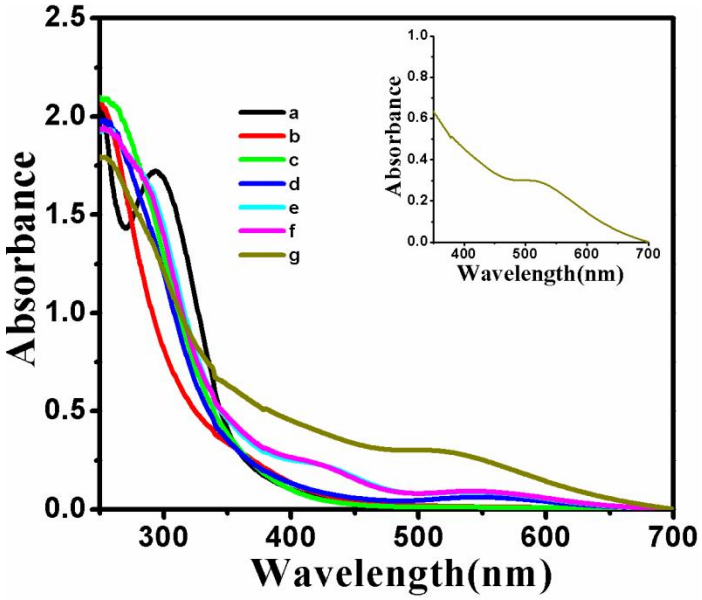

Figure. 4.5.UV-Vis spectra recorded on the sequential formation of Au-Pd from K_2PdCl_4 (20%) and $HAuCl_4$ (80%): the variation of absorbance of K_2PdCl_4 as a function of wavelength (a) followed by subsequent addition of 3-APTMS (b), THF-HPO (c), curve-d shows the spectra recorded after1 h, curve-e shows the absorption after subsequent addition of $HAuCl_4$ followed by addition of 3-APTMS (f), curve-g shows the spectra recorded after sequential formation of Au-Pd.

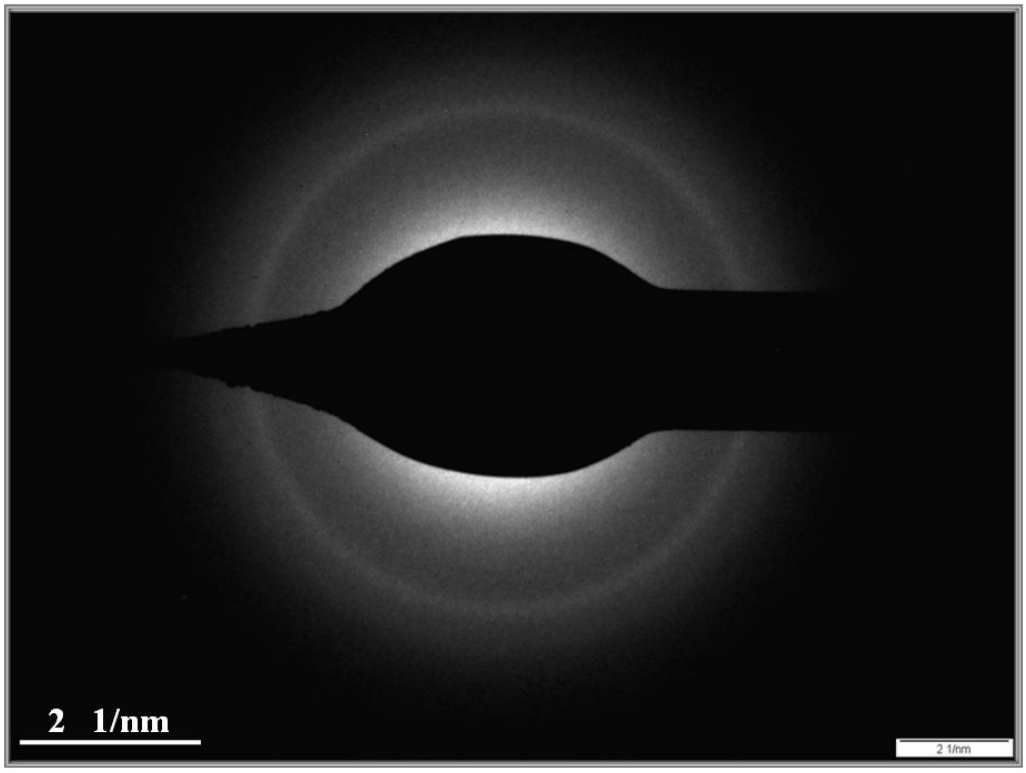

Figure. 4.6. SAED pattern of simultaneously synthesized Pd-Au.

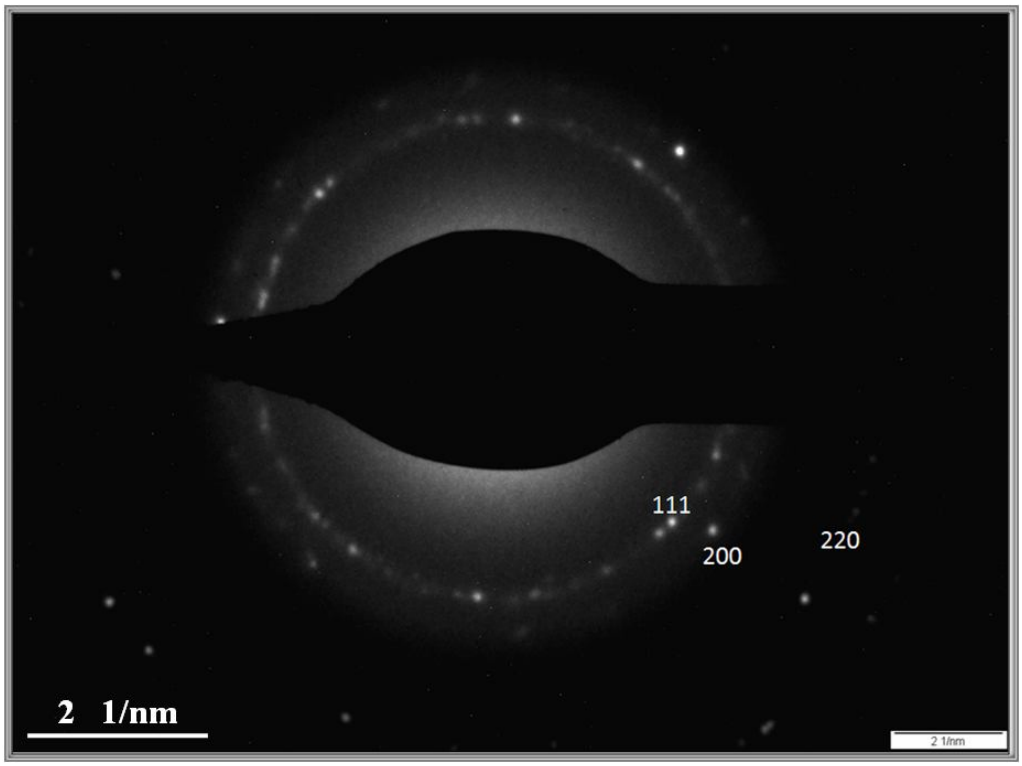

Figure. 4.7. SAED pattern of simultaneously synthesized Au-Pd.

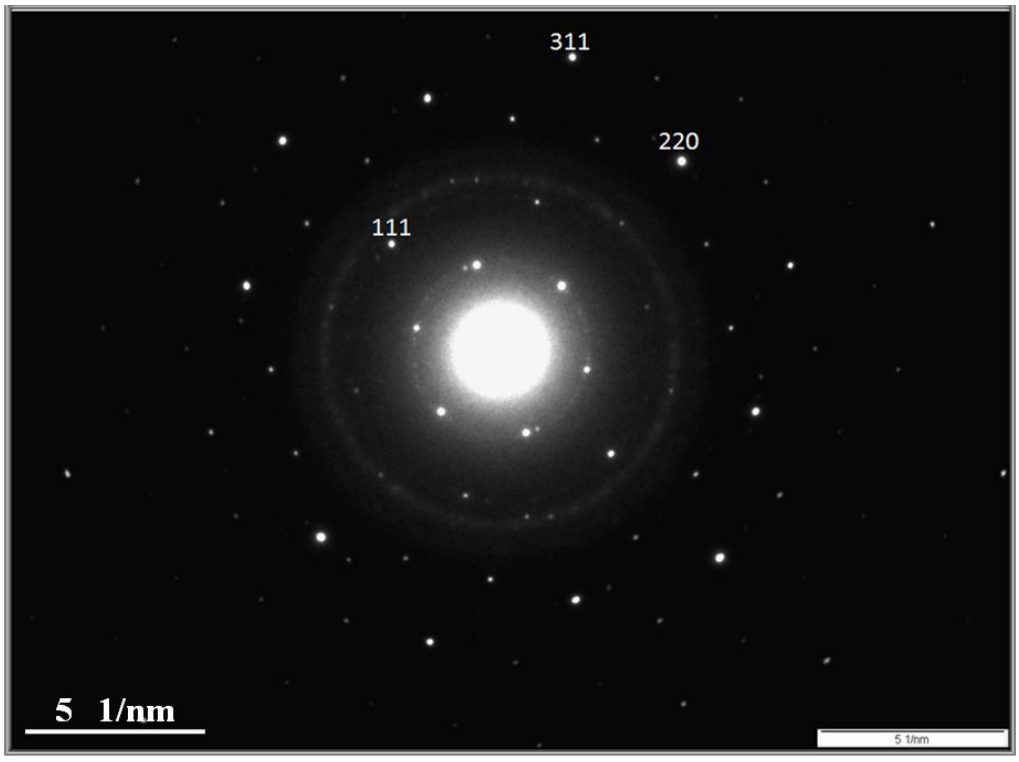

Figure. 4.8. SAED pattern of sequentially synthesized Pd-Au.

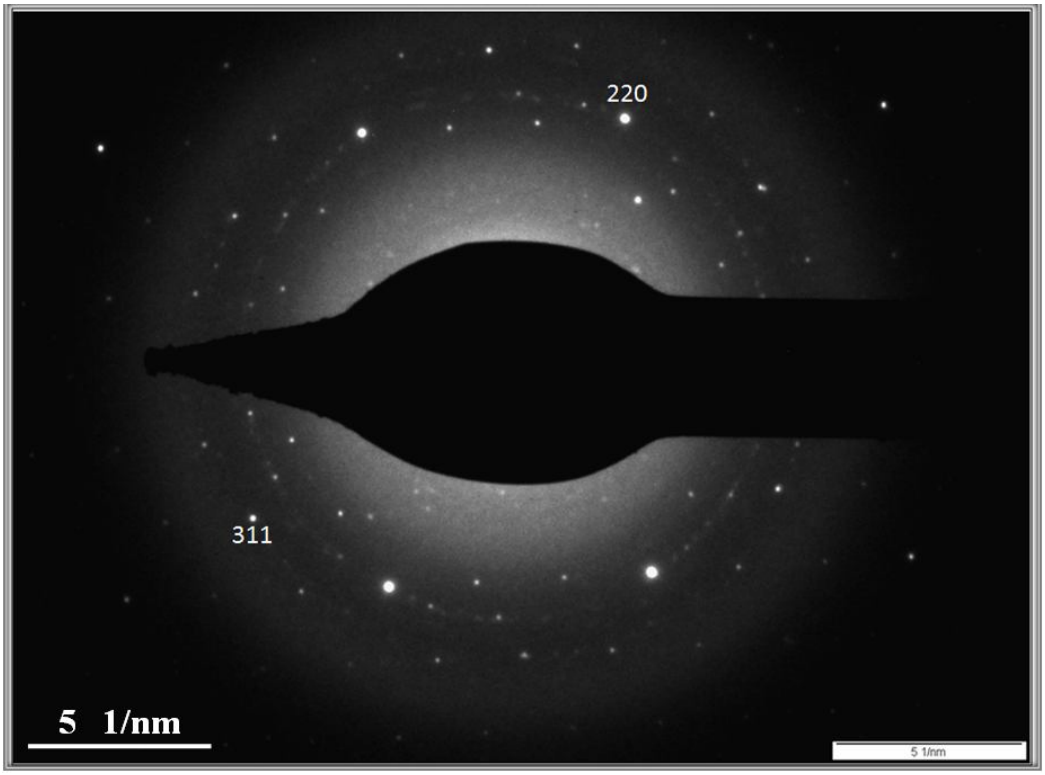

Figure. 4.9. SAED pattern of sequentially synthesized Au-Pd.

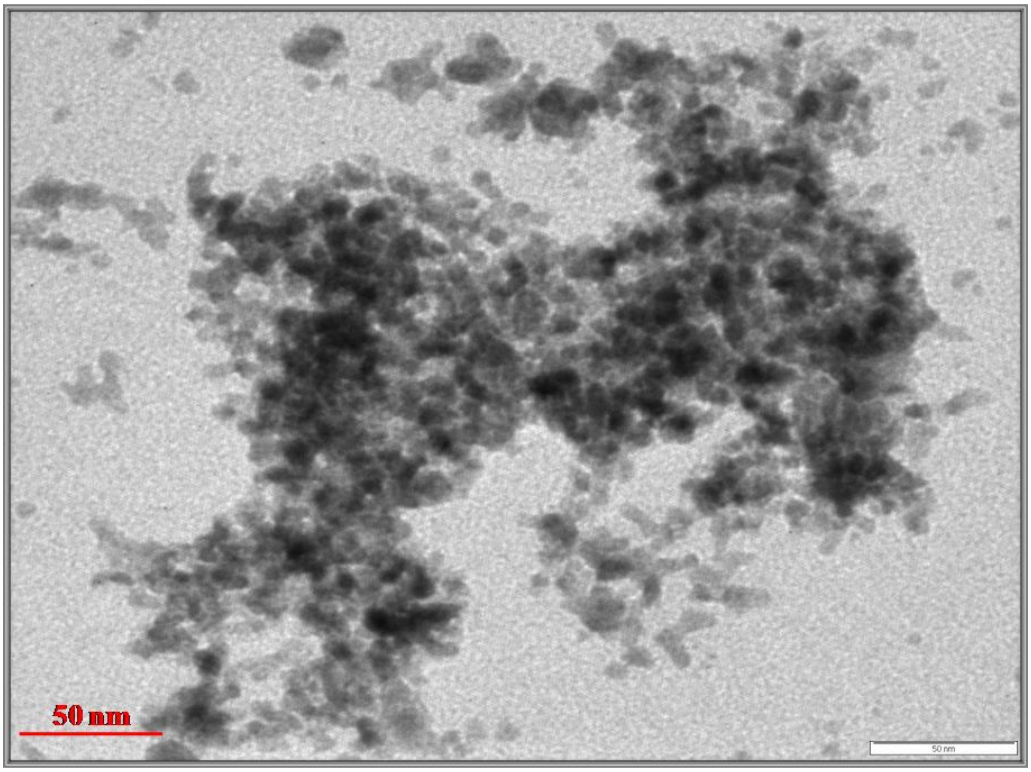

Figure. 4.10. TEM image of simultaneously synthesized Pd-Au.

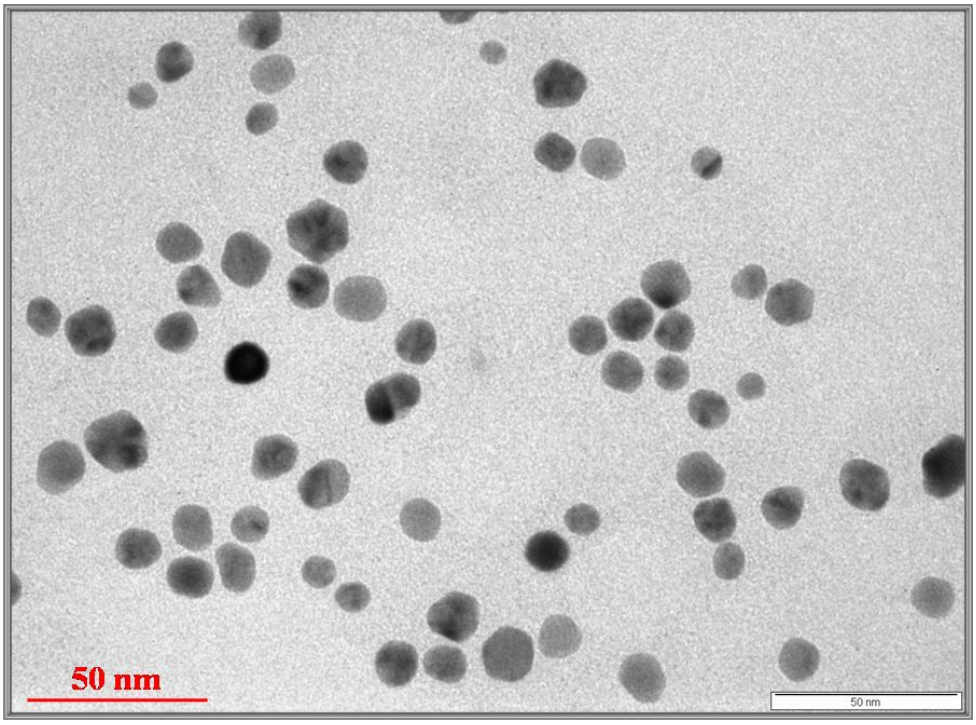

Figure. 4.11. TEM image of simultaneously synthesized Au-Pd.

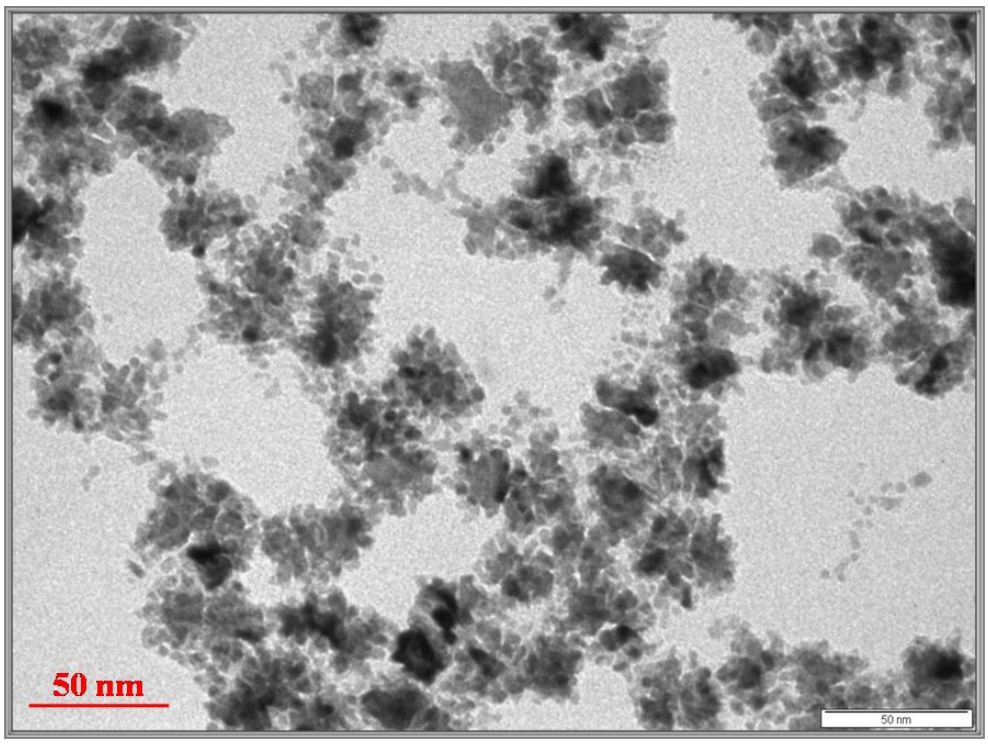

Figure. 4.12. TEM image of sequentially synthesized Pd-Au.

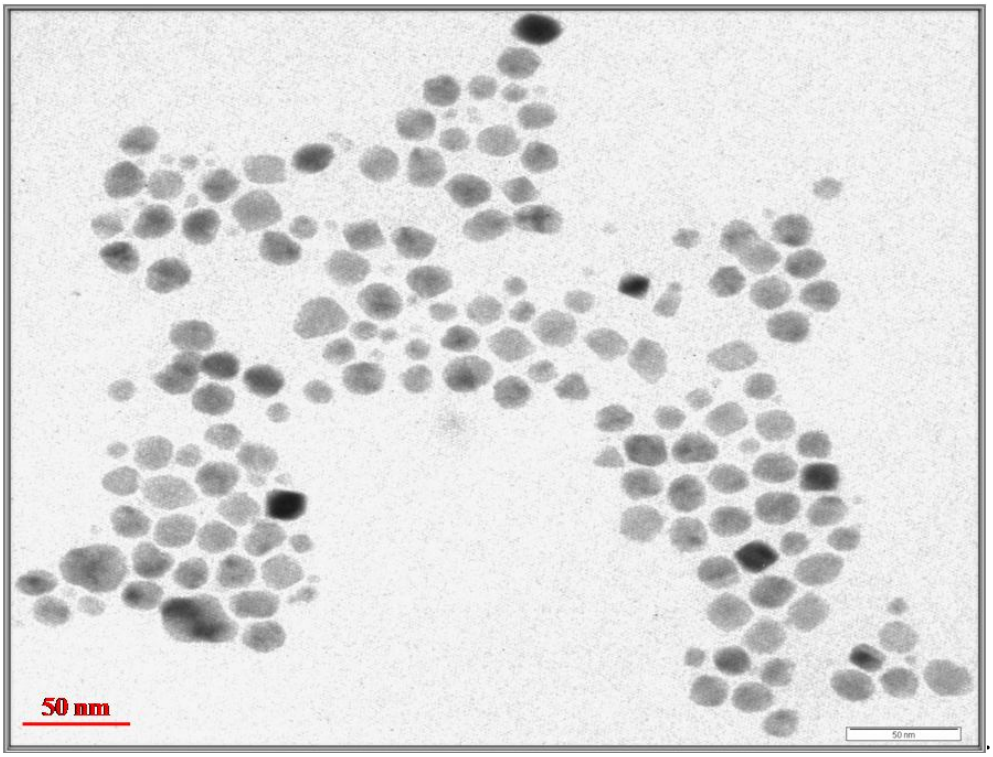

Figure. 4.13. TEM image of sequentially synthesized Au-Pd.

4.3.2. 3-APTMS and Cyclohexanone mediated synthesis of Ag-Au and Au-Ag

In previous section 2.2.2.2, 3-APTMS and cyclohexanone enable the synthesis of AgNPs. The similar reducing agents may also enable the synthesis of BMNPs of silver and gold. Figure 4.14 shows the visual photographs of BMNPs of Ag-Au and Au-Ag. The results based on UV-Vis spectroscopy on Ag-Au formation at two different ratios of Ag/Au i.e. 1/4 and 4/1 are shown in Figure 4.15(a),(b) and reveals the formation of BMNPs and the insets of Figure 4.15(a) and (b) shows the respective spectra for monometallic AuNPs and AgNPs respectively. Figure 4.16(a) shows the TEM image of Ag-Au (1/4) nanoparticles with an average particle size of 10.3 nm Figure 4.16 (b) and in Figure 4.17 the SAED pattern of the same clearly demonstrate the polycrystalline pattern of BMNPs.

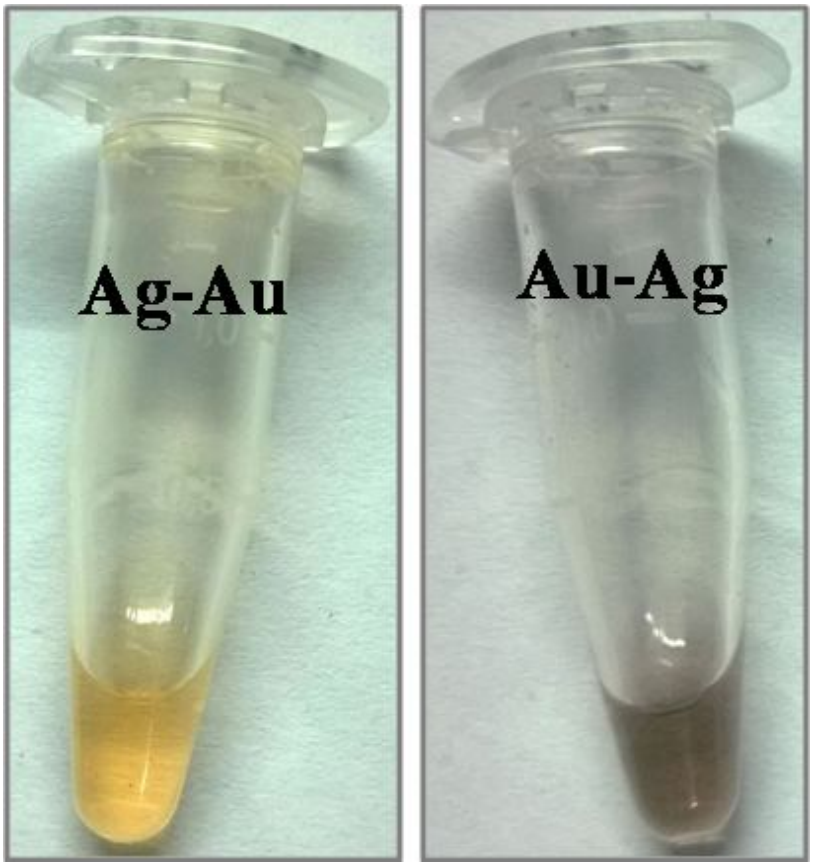

Figure. 4.14. The visual photographs of Ag-Au and Au-Ag.

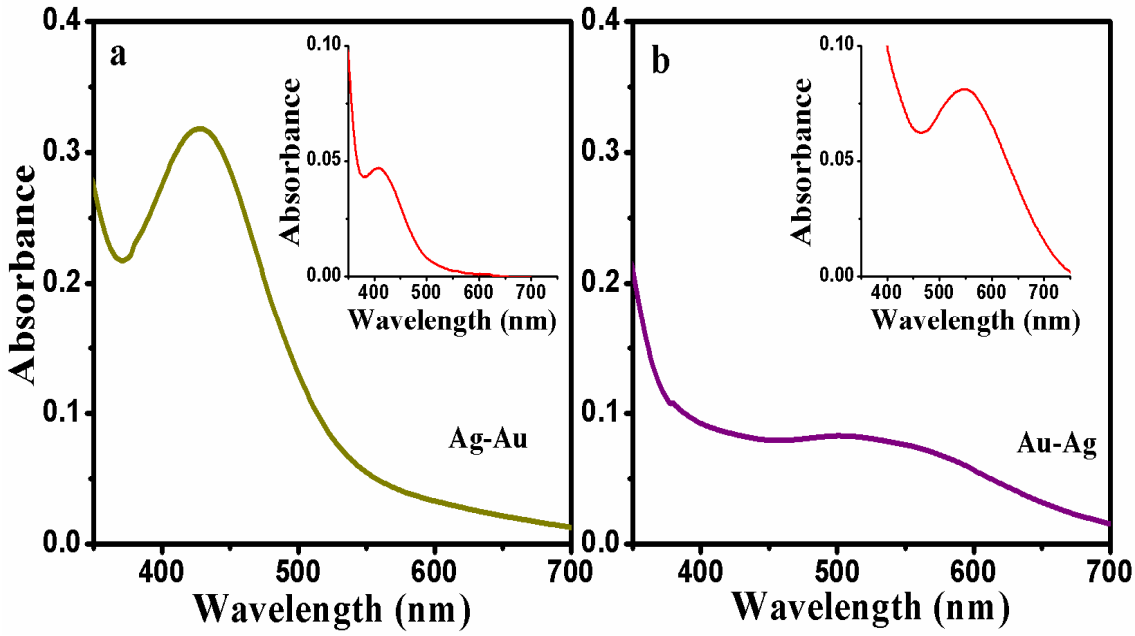

Figure. 4.15. The UV-Vis spectra of the corresponding Ag-Au and Au-Ag and the insets shows the UV-Vis spectra of monometallic AgNPs and AuNPs.

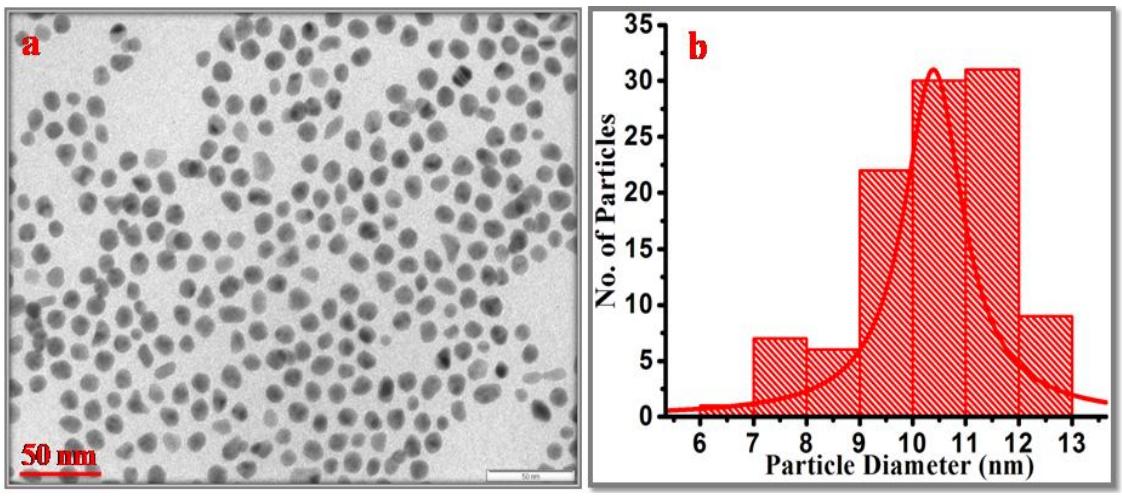

Figure. 4.16. (a) TEM image of Au-Ag, **(b)** particle size distribution.

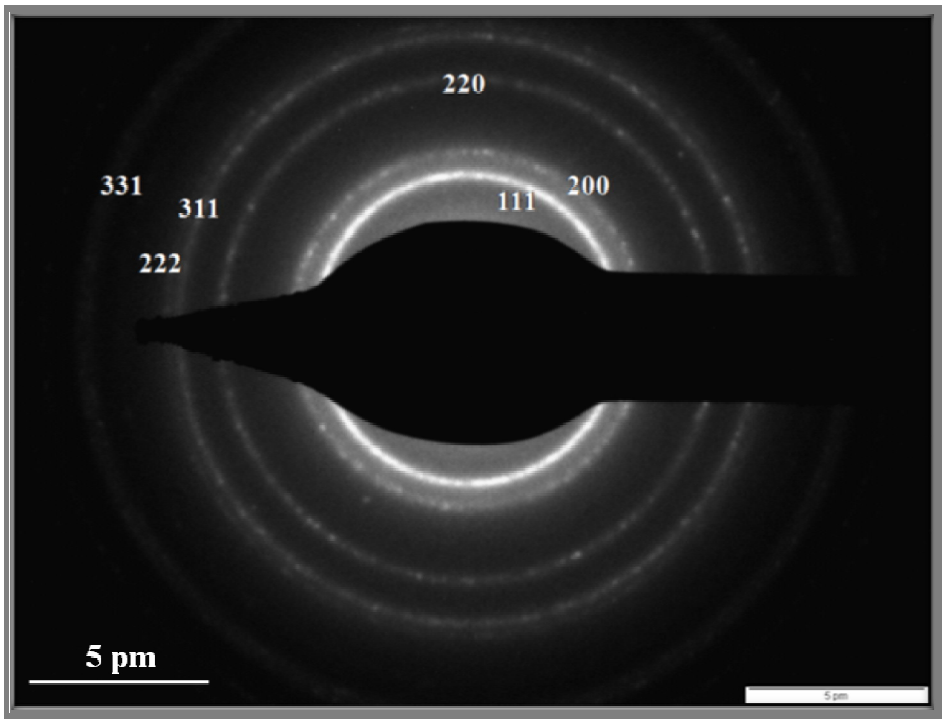

Figure. 4.17. SAED pattern of Au-Ag.

4.3.3. Cyclohexanone and 3-APTMS mediated synthesis of PBNP-AgNP/PBNP-Au-Ag nanocomposites

The advances in fine tuning of AgNPs/Au-Ag as biocomponent or multicomponent composites facilitates the catalytic activity of the resulting nanomaterial. Recently the role of 3-APTMS and cyclohexanone has been demonstrated in the synthesis of polycrystalline PBNP dispersion [Pandey and Pandey., (2013a)] providing a suitable host matrix for nanocomposite preparation. The results on the formation of the nanocomposite based on UV-Vis spectroscopy are shown in Figure 4.18 where the absorption spectra of $AgNP_5$, PBNP and PBNP-$AgNP_5$ are present and inset shows the visual photograph of the corresponding systems. Figure 4.19 shows the TEM image of PBNP-$AgNP_5$ with average particle size of 13 nm and Figure 4.20 shows SAED pattern clearly demonstrate the polycrystallinity of the nanocomposite. Further the effect of partial tuning between GPTMS and cyclohexanone has also been explored. Figure 4.21 shows the TEM image of PBNP-$AgNP_1$ with average particle size of 38 nm revealing the agglomeration of nanoparticles.

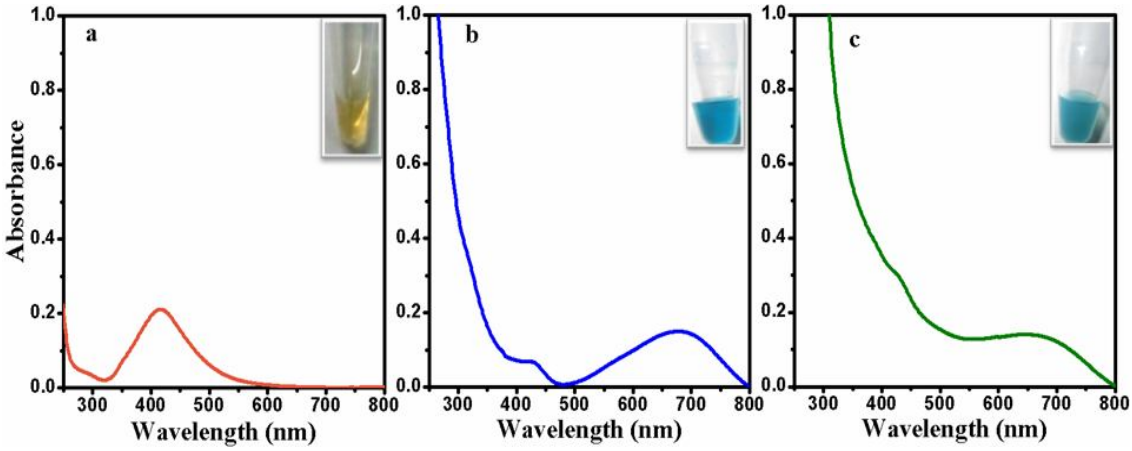

Figure. 4.18. UV-Vis spectra of (a) $AgNP_5$, (b) PBNP and (c) PBNP-$AgNP_5$; the inset shows the photographs of the corresponding system.

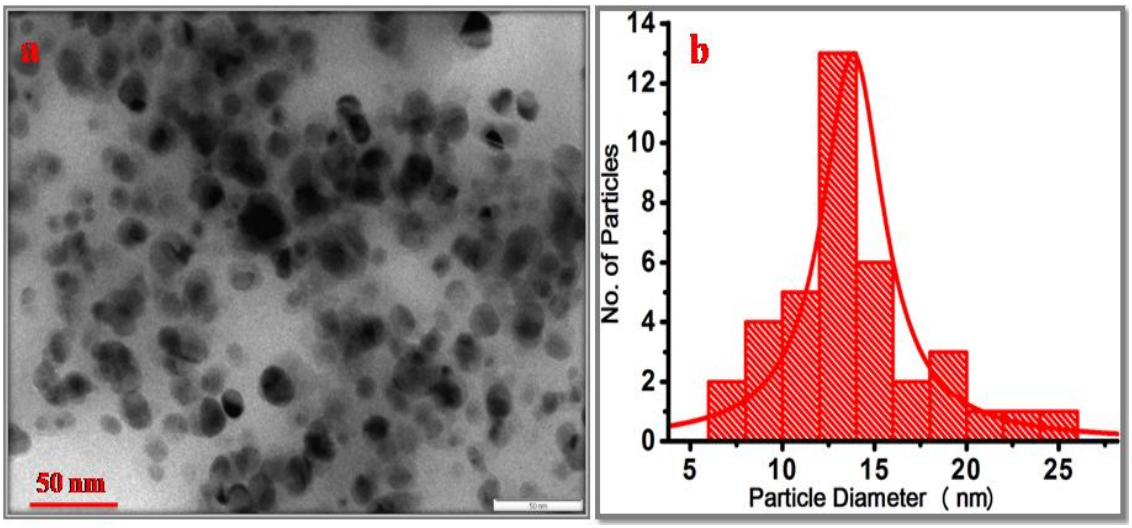

Figure. 4.19. (a) TEM image of PBNP-AgNP$_5$,**(b)** particle size distribution.

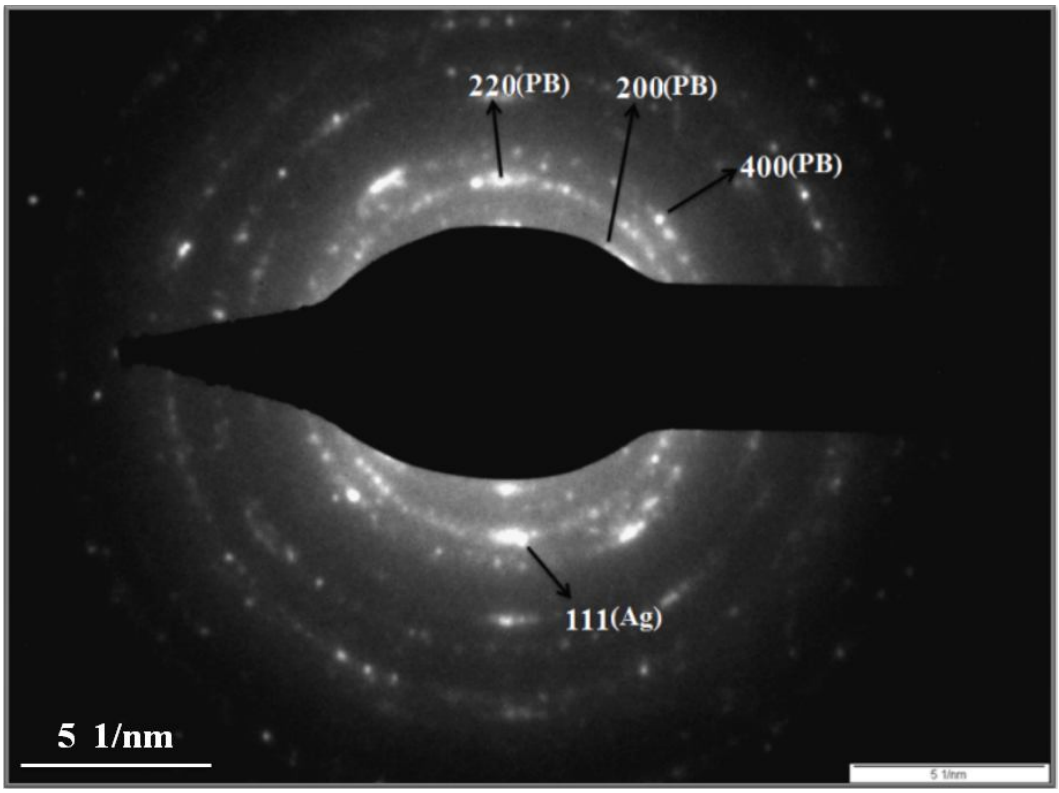

Figure. 4.20. SAED pattern of PBNP-AgNP$_5$.

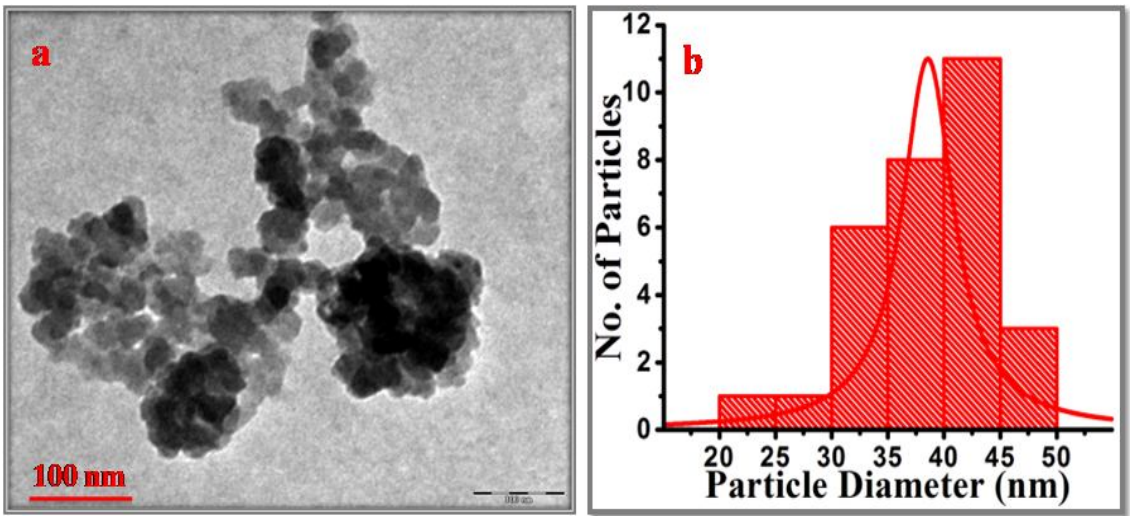

Figure. 4.21. (a) TEM image of PBNP-AgNP$_1$, **(b)** particle size distribution.

4.4. DISCUSSION

4.4.1.Tetrahydrofuran hydroperoxide and 3-APTMS mediated synthesis of Pd-Au and Au-Pd

3-APTMS and Tetrahydrofuran hydroperoxide are previously applicable for the synthesis of AuNPs [Pandey and Pandey., (2014c)] and PdNPs (in Chapter 3). In addition to that above process is also applicable for the synthesis of bimetallic nanoparticles of Pd-Au and Au-Pd under two different conditions; (1) Simultaneous and (2) Sequential. In simultaneous synthesis both palladium and gold salts are mixed together with reducing agents (3-APTMS andTHF-HPO) whereas in sequential method either PdNPs or AuNPs are synthesized first with reducing agents followed by allowing the formation of AuNPs or PdNPs thereafter on core-shell. The visual photographs of simultaneously synthesized Au-PdNPs and Pd-AuNPs as shown in Figure 4.1. A comparative study was made on the synthesis of bimetallic nanoparticles through simultaneous and sequentially. The major findings recorded during the simultaneous and sequential synthesis of nanoparticles are as follows: (1) Pd-Au nanoparticles made through simultaneous method shows disappearance of absorption at 530 nm (inset of Figure 4.2) which is characteristics of AuNPs when 80:20 ratios of Pd and Au. (2) Au-Pd nanoparticles made through simultaneous method shows intense absorption at 530 nm (inset of Figure 4.3) when 20:80 ratio of

Pd and Au salt. (3) Pd-Au made through sequentially under similar condition as in (1) shows a plateau justifying sign of AuNPs (inset of Figure 4.4) when 80:20 ratio of Pd and Au, and (4) Au-Pd made through sequentially under similar condition as in (2) shows less intense sign of AuNPs (inset of Figure 4.5) 20:80 ratios of Pd and Au salt.

Further insight on such interaction which has been discussed in previous section 3.4.1. also confirmed during the synthesis of bimetallic nanoparticles of Pd-Au and Au-Pd through simultaneous and sequential process. Figure 4.6 and 4.7 shows SAED pattern of Pd-Au and Au-Pd BMNPs synthesized by simultaneous process and Figure 4.8 and 4.9 shows SAED pattern of Pd-Au and Au-Pd BMNPs synthesized by sequential method. The results clearly demonstrate the occurrence of excellent polycrystalline pattern as shown in Figure 4.8-9 when nanoparticles formation takes place through sequential, while on the other hand simultaneous synthesis of the same (Pd-Au or Au-Pd) as shown in Figure 4.6-7 enable decrease in polycrystallinity. In previous section 3.4.1 PdNPs has affinity for interaction with silanol moiety whereas AuNPs formed under similar conditions do not show such behavior. Therefore simultaneous synthesis of PdNPs having more palladium contents results significantly decrease in polycrystallinity as a function of silanol concentration (Figure 4.6) whereas an increase in gold content under similar condition results relatively less decrease of the same (Figure 4.7). Under sequential process of BMNPs synthesis when palladium is reduced first, formation of bimetallic nanoclusters takes place that restrict any further interaction with silanol moiety causing significant increase in polycrystallinity of the materials (Figure 4.8-9). The electron diffraction pattern of Au-Pd (simultaneous) as shown in Figure 4.7 were indexed with the (111), (200) and (220) lattice planes with spacing 0.223 nm and 0.192 nm , while SAED pattern of Pd-Au sequential as shown in Figure 4.8 were (111), (220) and (311) lattice planes with spacing 0.235 nm,0.139 nm and 0.122 nm. Further the electron diffraction pattern of Au-Pd (sequential) indexed with (220) and (311) lattice planes with d-spacing 0.142 nm and 0.122 nm as shown in Figure 4.9.

Subsequently we further investigated the morphology and size of as synthesized BMNPs through TEM images as shown in Figure 4.10-13. These SAED

and TEM images clearly demonstrate following major findings: (1) simultaneous synthesis of bimetallic nanoparticles causes decrease in polycrystallinity; (2) when palladium ions are reduced first, formation of bimetallic clusters is observed whereas initial reduction of gold ions causes aggregation of same forming larger nanoparticles. The aggregation on initial reduction of gold ions during the formation of bimetallic nanoparticles and bimetallic nanoclusters has been reported by Toshima *et al* [Harada *et al*., (1993); Toshima and Yonezawa., (1998)]. However decrease in polycrystallinity during simultaneous synthesis of bimetallic nanoparticles need to be reviewed precisely.

4.4.2. Cyclohexanone and 3-APTMS mediated synthesis of Ag-Au and Au-Ag

Cyclohexanone and 3-APTMS are the potential candidates for the synthesis of NMNPs [Pandey *et al*., (2014b)]. Similar process for the conversion of 3-APTMS capped bimetallic (Ag^{+} and Au^{3+}) ions by cyclohexanone is observed. When silver salt:gold salt ratio is 4:1, it has been found that cyclohexanone on mixing with 3-APTMS capped Ag^{+}:Au^{3+} ions immediately converted into a yellow solution which subsequently leads into Ag-Au BMNPs. While silver salt:gold salt ratio is 1:4, cyclohexanone on mixing with 3-APTMS capped metal ions immediately converted into a magenta colour which subsequently leads into Au-Ag BMNPs. The observations based on UV-Vis spectroscopy and imaging photography justify the conversion of silver nitrate and auric chloride into bimetallic Ag-Au/Au-Ag nanoparticles (Figure 4.14-15).

The morphology of bimetallic Au-Ag (Figure 4.16), evaluated by the TEM as shown in Figure 4.17. It shows circular morphology and well monodisperse with 10.3 nm average particle size (Figure 4.16). In order to understand, the SAED pattern of Au-Ag are recorded in Figure 4.17. The electron diffraction pattern exhibited six rings assigned to (111), (200), (220), (311), (222) and (331) lattice planes with spacing 0.220 nm, 0.191 nm, 0.134 nm, 0.114 nm, 0.110 nm and 0.087 nm are observed which may be indexed based on the fcc structures of silver and gold.

4.4.3. Nanocomposites of PBNP-AgNP or PBNP-Au-Ag synthesized by Cyclohexanone and 3-APTMS

The use of the same reducing agents (Cyclohexanone and 3-APTMS) making the AgNPs/Au-Ag and functional host like PBNP may facilitate the formation of nanocomposite. The observations based on UV-Vis spectroscopy and imaging photography justify that the presence of hump at 419 nm (characteristics of $AgNP_5$) and maxima at 640 nm (characteristics of PBNP) shows the characteristics of nanocomposite as shown in Figure 4.18 (c). The visual photograph of nanocomposite also revealed the best tuning of AgNPs and PBNPs during nanocomposite formation (inset of Figure 4.18 c). The finding based on TEM image of PBNP-$AgNP_5$ shows circular morphology and uniformly dispersed nanoparticles with average particle size of 13 nm (Figure 4.19). Its electron diffraction pattern clearly demonstrates the polycrystallinity and lattice planes reveal the presence of AgNP and PBNP. The pattern indexed with (200), (220) and (400) of PBNP and (111) of AgNP reveals that the nanocomposite consisting both the nature of PBNP and AgNP (Figure 4.20).

Further the nanocomposite formation takes place in the presence of PBNP and AgNP where AgNP is synthesized with the help of 3-APTMS and GPTMS (replacing cyclohexanone), there is partial tuning in between AgNPs and PBNP due to the presence of GPTMS which is hydrophobic in nature, also increases the viscosity of the medium revealing the tendency for the agglomeration of the nanoparticles as well as size become 38 nm and also there is absence of uniform dispersion (Figure 4.21a, and b).

4.5. CONCLUSION

The findings reported in this chapter demonstrated the followings: (1) Bimetallic nanoparticles of Pd-Au and Au-Pd are made through 3-APTMS and THF-HPO mediated conversion of respective noble metal salts; (2) The BMNPs of Pd-Au and Au-Pd justifies potential affinity of PdNPs with silanol group whereas AuNPs do not show such affinity; (3) When palladium ions are reduced first, formation of

bimetallic clusters is observed whereas initial reduction of gold ions causes aggregation of same forming larger nanoparticles; (4) Formation of bimetallic nanoclusters tends to decrease the silanol interaction justifying an increase in polycrystallinity as compared to that of the same under simultaneous synthesis of bimetallic nanoparticles; (5) BMNPs of Ag-Au or Au-Ag using cyclohexanone and 3-APTMS exhibit improved catalytic performance because of both synergistic and electronic effects; and (6) The use of similar reducing agents also enables the synthesis of polycrystalline PBNPs that allows the formation of nanostructured composites with a crystallized framework.